Jessen, Miller et al., "MEK Inhibition Exhibits Efficacy in Human and Mouse Neurofibromatosis Tumors"

SUPPLEMENTAL INFORMATION

Supplemental Tables

Supplemental Table S1 (related to Supplemental Figure S1). Microarray samples grouped by sample type. Column 1 = sample number; Column 2 = data file name; Column 3 = hybridization probe sample number; Column 4 = hybridization batch; Column 5 = mouse genotype or human tumor type; Column 6 = sample type (*Mus musculus*; hs = *Homo sapiens*).

MOUSE SAMPLE SET (MM CONTROL VS MM NEUROFIBROMA VS MM MPNST) --note that each sample type contains a m of 3 samples N = nerve; T = tumor					
27	HybI-N17_MOE430_2.CEL	N17	HybI	P0CreB	mm control
35	HybH-N19_MOE430_2.CEL	N19	HybH	P0CreB	mm control
44	HybG-N18_MOE430_2.CEL	N18	HybG	P0CreB	mm control
50	HybE-N16_MOE430_2.CEL	N16	HybE	P0CreB	mm control
58	HybD-N15_MOE430_2.CEL	N15	HybD	P0CreB	mm control
30	HybI-N03_MOE430_2.CEL	N03	HybI	Nf1 flox/flox	mm control
38	HybH-N05_MOE430_2.CEL	N05	HybH	Nf1 flox/flox	mm control
46	HybG-N04_MOE430_2.CEL	N04	HybG	Nf1 flox/flox	mm control
53	HybE-N02_MOE430_2.CEL	N02	HybE	Nf1 flox/flox	mm control
61	HybD-N01_MOE430_2.CEL	N01	HybD	Nf1 flox/flox	mm control
28	HybI-N12_MOE430_2.CEL	N12	HybI	Nf2 flox/flox	mm control
36	HybH-N14_MOE430_2.CEL	N14	HybH	Nf2 flox/flox	mm control
45	HybG-N13_MOE430_2.CEL	N13	HybG	Nf2 flox/flox	mm control
51	HybE-N11_MOE430_2.CEL	N11	HybE	Nf2 flox/flox	mm control
59	HybD-N10_MOE430_2.CEL	N10	HybD	Nf2 flox/flox	mm control
63	HybC-T3_MOE430_2.CEL	T3	HybC	T-P0CreB; Nf1 flox/flox	mm neurofibroma
72	HybB-T2_MOE430_2.CEL	T2	HybB	T-P0CreB; Nf1 flox/flox	mm neurofibroma
79	HybA-T4_MOE430_2.CEL	T4	HybA	T-P0CreB; Nf1 flox/flox	mm neurofibroma
81	HybA-T1_MOE430_2.CEL	T1	HybA	T-P0CreB; Nf1 flox/flox	mm neurofibroma

2	HybM-T12_MOE430_2.CEL	T12	HybM	T-DhhCre; Nf1 flox/-	mm neurofibroma
3	HybM-T11_MOE430_2.CEL	T11	HybM	T-DhhCre; Nf1 flox/-	mm neurofibroma
20	HybJ-T13_MOE_430_2.CEL	T13	HybJ	T-DhhCre; Nf1 flox/-	mm neurofibroma
21	HybJ-T10_MOE_430_2.CEL	T10	HybJ	T-DhhCre; Nf1 flox/-	mm neurofibroma
1	HybM-T4_MOE430_2.CEL	T4	HybM	T-DhhCre; Nf1 flox/flox	mm neurofibroma
18	HybJ-T6_MOE_430_2.CEL	T6	HybJ	T-DhhCre; Nf1 flox/flox	mm neurofibroma
19	HybJ-T1_MOE_430_2.CEL	T1	HybJ	T-DhhCre; Nf1 flox/flox	mm neurofibroma
22	HybI-T29_MOE430_2.CEL	T29	HybI	T-DhhCre; Nf1 flox/flox	mm neurofibroma
23	HybI-T28_MOE430_2.CEL	T28	HybI	T-DhhCre; Nf1 flox/flox	mm neurofibroma
24	HybI-T27_MOE430_2.CEL	T27	HybI	T-DhhCre; Nf1 flox/flox	mm neurofibroma
25	HybI-T26_MOE430_2.CEL	T26	HybI	T-DhhCre; Nf1 flox/flox	mm neurofibroma
62	HybC-T7_MOE430_2.CEL	T7	HybC	T-P0CreB; Nf2 flox/flox	mm mpnst
71	HybB-T6_MOE430_2.CEL	T6	HybB	T-P0CreB; Nf2 flox/flox	mm mpnst
78	HybA-T5_MOE430_2.CEL	T5	HybA	T-P0CreB; Nf2 flox/flox	mm mpnst
68	HybC-T12_MOE430_2.CEL	T12	HybC	T-P0CreB; Nf2 flox/+; Nf1 flox/flox	mm mpnst
69	HybC-T10_MOE430_2.CEL	T10	HybC	T-P0CreB; Nf2 flox/+; Nf1 flox/flox	mm mpnst
70	HybB-T9_MOE430_2.CEL	T9	HybB	T-P0CreB; Nf2 flox/+; Nf1 flox/flox	mm mpnst
76	HybB-T11_MOE430_2.CEL	T11	HybB	T-P0CreB; Nf2 flox/+; Nf1 flox/flox	mm mpnst
77	HybA-T8_MOE430_2.CEL	T8	HybA	T-P0CreB; Nf2 flox/+; Nf1 flox/flox	mm mpnst
67	HybC-T15_MOE430_2.CEL	T15	HybC	T-P0CreB; Nf2 flox/flox; Nf1 flox/+	mm mpnst
75	HybB-T16_MOE430_2.CEL	T16	HybB	T-P0CreB; Nf2 flox/flox; Nf1 flox/+	mm mpnst
83	HybA-T13_MOE430_2.CEL	T13	HybA	T-P0CreB; Nf2 flox/flox; Nf1 flox/+	mm mpnst
66	HybC-T19_MOE430_2.CEL	T19	HybC	T-P0CreB; Nf2 flox/flox; p53+/-	mm mpnst
74	HybB-T18_MOE430_2.CEL	T18	HybB	T-P0CreB; Nf2 flox/flox; p53+/-	mm mpnst
82	HybA-T17_MOE430_2.CEL	T17	HybA	T-P0CreB; Nf2 flox/flox; p53+/-	mm mpnst
64	HybC-T25_MOE430_2.CEL	T25	HybC	T-NPcis	mm mpnst
65	HybC-T23_MOE430_2.CEL	T23	HybC	T-NPcis	mm mpnst
73	HybB-T22_MOE430_2.CEL	T22	HybB	T-NPcis	mm mpnst
80	HybA-T21_MOE430_2.CEL	T21	HybA	T-NPcis	mm mpnst
HUMAN SAMPLE SET (HS NERVE VS NS NF VS HS MPNST) -- colors indicate genotype groups (note that each contains a min of 3 samples)					
86	jan-N3_HG_U133_Plus_2#2.CEL	N3	jan	nerve	hs nerve
87	jan-N2_HG_U133_Plus_2#2.CEL	N2	jan	nerve	hs nerve

88	jan-N1_HG_U133_Plus_2#2.CEL	N1	jan	nerve	hs nerve
90	batch3c-dNF_AS50_HG_U13Plus_2.CEL	AS50	batch3c	dNF	hs NF
95	batch3c-DNF_LRS_HG_U13Plus_2.CEL	LRS	batch3c	dNF	hs NF
99	batch3b-dNF_CSG95_HG_U133_Plus_2.CEL	CSG95	batch3b	dNF	hs NF
101	batch3b-dNF_CSG94_HG_U133_Plus_2.CEL	CSG94	batch3b	dNF	hs NF
109	batch3a-dNF_AS55_HG_U133_Plus_2.CEL	AS55	batch3a	dNF	hs NF
120	batch2c-dNF.AS44_HG_U133_Plus_2.CEL	AS44	batch2c	dNF	hs NF
122	batch2c-dNF.AS35_HG_U133_Plus_2.CEL	AS35	batch2c	dNF	hs NF
136	batch2b-dNF.AS4_HG_U133_Plus_2.CEL	AS4	batch2b	dNF	hs NF
138	batch2b-dNF.AS22_HG_U133_Plus_2.CEL	AS22	batch2b	dNF	hs NF
152	batch2a-dNF.AS46_HG_U133_Plus_2.CEL	AS46	batch2a	dNF	hs NF
154	batch2a-dNF.AS3_HG_U133_Plus_2.CEL	AS3	batch2a	dNF	hs NF
188	batch1a-dNF_AS5_HG_U133_Plus_2.CEL	AS5	batch1a	dNF	hs NF
190	batch1a-dNF_AS18_HG_U133_Plus_2.CEL	AS18	batch1a	dNF	hs NF
105	batch3a-pNF_AS48_HG_U133_Plus_2.CEL	AS48	batch3a	pNF	hs NF
114	batch2c-pNF.AS34_HG_U133_Plus_2.CEL	AS34	batch2c	pNF	hs NF
116	batch2c-pNF.AS33_HG_U133_Plus_2.CEL	AS33	batch2c	pNF	hs NF
118	batch2c-pNF.AS32_HG_U133_Plus_2.CEL	AS32	batch2c	pNF	hs NF
130	batch2b-pNF.AS47_HG_U133_Plus_2.CEL	AS47	batch2b	pNF	hs NF
132	batch2b-pNF.AS24_HG_U133_Plus_2.CEL	AS24	batch2b	pNF	hs NF
134	batch2b-pNF.AS23_HG_U133_Plus_2.CEL	AS23	batch2b	pNF	hs NF
146	batch2a-pNF.AS40_HG_U133_Plus_2.CEL	AS40	batch2a	pNF	hs NF
148	batch2a-pNF.AS38_HG_U133_Plus_2.CEL	AS38	batch2a	pNF	hs NF
150	batch2a-pNF.AS12_HG_U133_Plus_2.CEL	AS12	batch2a	pNF	hs NF
182	batch1a-pNF_AS8_HG_U133_Plus_2.CEL	AS8	batch1a	pNF	hs NF
184	batch1a-pNF_AS7_HG_U133_Plus_2.CEL	AS7	batch1a	pNF	hs NF
186	batch1a-pNF_AS16_HG_U133_Plus_2.CEL	AS16	batch1a	pNF	hs NF
127	batch2c-MPNST.AS45_HG_U133_Plus_2.CEL	AS45	batch2c	MPNST	hs MPNST
143	batch2b-MPNST.AS42_HG_U133_Plus_2.CEL	AS42	batch2b	MPNST	hs MPNST
158	batch2a-MPNST.AS37_HG_U133_Plus_2.CEL	AS37	batch2a	MPNST	hs MPNST
192	batch1a-MPNST_AS15_HG_U133_Plus_2.CEL	AS15	batch1a	MPNST	hs MPNST
194	batch1a-MPNST_AS13_HG_U133_Plus_2.CEL	AS13	batch1a	MPNST	hs MPNST
196	batch1a-MPNST_AS10_HG_U133_Plus_2.CEL	AS10	batch1a	MPNST	hs MPNST

Supplemental Table S2 (related to Supplemental Figure S1). Detailed cluster annotation: genes and associated biological themes in clusters C17 - C20 (Supplemental Figure S1A). NF = neurofibroma; MPNST = malignant peripheral nerve sheath tumor. Ortholog number refers to the number of gene orthologs represented in each cluster. Biological themes represented in each cluster are defined by DAVID. Genes from represented biological themes are listed alphabetically.

luster		Ortholog #	Biological Themes	Cluster genes that annotate to biological themes
C17	Up in NF	398	Axonogenesis, Glycolysis, Induction of apoptosis, Negative regulation of JAK-STAT cascade, Negative regulation of MAP kinase activity, Regulation of cell adhesion, Regulation of neurotransmitter levels, Sphingolipid metabolism	APOE, ARHGDIB, ARHGDIG, BID, CADM1, CDKN2A, CXCR4, DUSP6, EFNA5, FXYD5, HEXB, HPRT1, KCNMA1, LIN7B, MDH1, MDH2, NRXN2, NUMBL, PKM2, PMAIP1, PPP2CA, PPP2R1A, PTPRZ1, PYCARD, RHOC, SEMA4F, SLITRK4, SLITRK6, SNPH, SPRED2, SPRY2, SPRY4, ST8SIA1, STK17B, TGFB2, THY1, TNFRSF12A, TRAF3
C18	Down in NF	414	Actomyosin structure organization and biogenesis, Cellular lipid metabolism, Negative regulation of progression through cell cycle, Peripheral nervous system development	ABCA2, ACOX2, ADIPOQ, AGT, ATM, CAV3, CD36, CDKN1C, CEL, CYB5R2, FA2H, FAAH, FAR1, GAS2L3, HEPACAM, HSD17B14, ILKAP, KRT19, LCAT, LEP, LPL, LSS, LTC4S, MYH11, NF1, PCK1, PDSS1, PIP5K1A
C19	Up in MPNST	1016	Apoptosis, DNA repair, DNA replication, Glycosaminoglycan metabolism, Golgi vesicle transport, Negative regulation of MAP kinase activity, Phosphoinositide-mediated signaling, Regulation of mitosis	ACVR1, ANLN, ANXA5, APEX1, APLP1, ARCN1, ARF4, ARF6, AURKA, B3GALT6, B4GALT1 BAX, BCL2L11, BID, BIRC5, BUB1, BUB1B, C11orf82, C5AR1, CASP3, CASP6, CCNA2, CCNE1, CD3E, CDC2, CDC25C, CDC45L, CDC6, CDC7, CDKN2C, CDT1, CENPF, CHAF1B, CHEK1, CHST11, CHST13, CKAP2, CLSPN, COPA, COPB2, COPE, COPG, COPZ1, CRY1, CTSB, DAD1, DAP, DBF4, DTL, DUSP6, DUSP9, DUT, E2F1, E2F2, EDN2, EDNRA, EGLN3, EIF2AK2, EME1, ERCC8, EREG, ERGIC1, ESCO2, ESPL1, EXO1, EXT1, F2R, FCER1G, FEN1, GADD45A, GALNS, Gene symbol, GINS1, GMNN, GNB2L1, GNS, GOSR2, GTSE1, GUSB, H2AFX, HEXA, HS2ST1, HSP90B1, HSPE1, HUS1, IER3, IGFBP3, INHBA, KIF20B, KIF22, KNTC1, LGALS1, LIN9, LITAF, LPAR2, MAD2L1, MAD2L1BP, MCFD2, MCM10, MCM2, MCM4, MCM5, MCM6, MCM7, NDC80, NEIL3, NEK2, NGFRAP1, NRAS, NRBP1, NUDT1, NUP62, NUSAP1, PDIA3, PECR, PIK3R2, PMAIP1, POLA1, POLD2, POLE2, POLH, PPP2CA, PPP2R1A, PRDX2, PRIM1, PRIM2, PTRH2, PTTG1, PYCARD, RAD18, RAD23B, RAD51, RAD51C, RAD54B, RFC2, RFC3, RFC4, RFC5, RPA2, RPA3, RRM1, RRM2, RUNX3, RUVBL2, SCAMP3, SEC24D, SERPINB2, SGPL1, SHFM1, SIAH2, SPAG5, SPRED2, SPRY2, SSRP1, STEAP2, STK17B, TBX3, TGFB2, TK1, TNFAIP8, TNFRSF10B, TNFRSF12A, TNFRSF21, TNFSF9, TOP2A, TRAF4, TRIAP1, TSPO, TTK, TXNL1, TYMS, UBA1, UBE2C, UNC5A, UNC5B, UPF1, VEGFA, XRCC1, XRCC5, YARS, YIPF5, YKT6
C20	Down in MPNST	758	Axon ensheathment, Axonogenesis, Catecholamine metabolism, Cellular lipid metabolism, Cholesterol transport, Fatty acid metabolism, Peripheral nervous system development, Pyruvate metabolism	ABCA2, ACSL1, ACSM5, ADIPOQ, AGPAT3, AGPAT9, ALDH3A2, ANGPTL3, APBB1, BDH2, CAV1, CD36, CD9, CHPT1, CNP, COMT, CYB5R2, CYP2J2, CYP46A1, DHCR24, ELOVL1, FA2H, FAAH, FADS1, FAR1, FCER1A, FEZ1, FEZ2, GGT5, GPT, HACL1, HDC, HSD17B14, HSD17B8, LASS4, LCAT, LEP, LPL, LRRC4C, LSS, MAL, MAOA, MBP, ME3, MPZ, NF1, NPC1, NR4A2, NTNG1, NTRK3, OSBPL1A, OSBPL5, PCK1, PIGB, PIK3R1, PIKFYVE, PIP4K2A, PLXNB1, PMP22, PPAP2A, PPARA, PPARGC1A, PRX, PTGDS, PYROXD2, RARRES2, RELN, RTN4RL1, S100B, SBF2, SCD, SEMA3B, SNCA, ST3GAL6, STX12, TIAM1 UGT8

Supplemental Figures

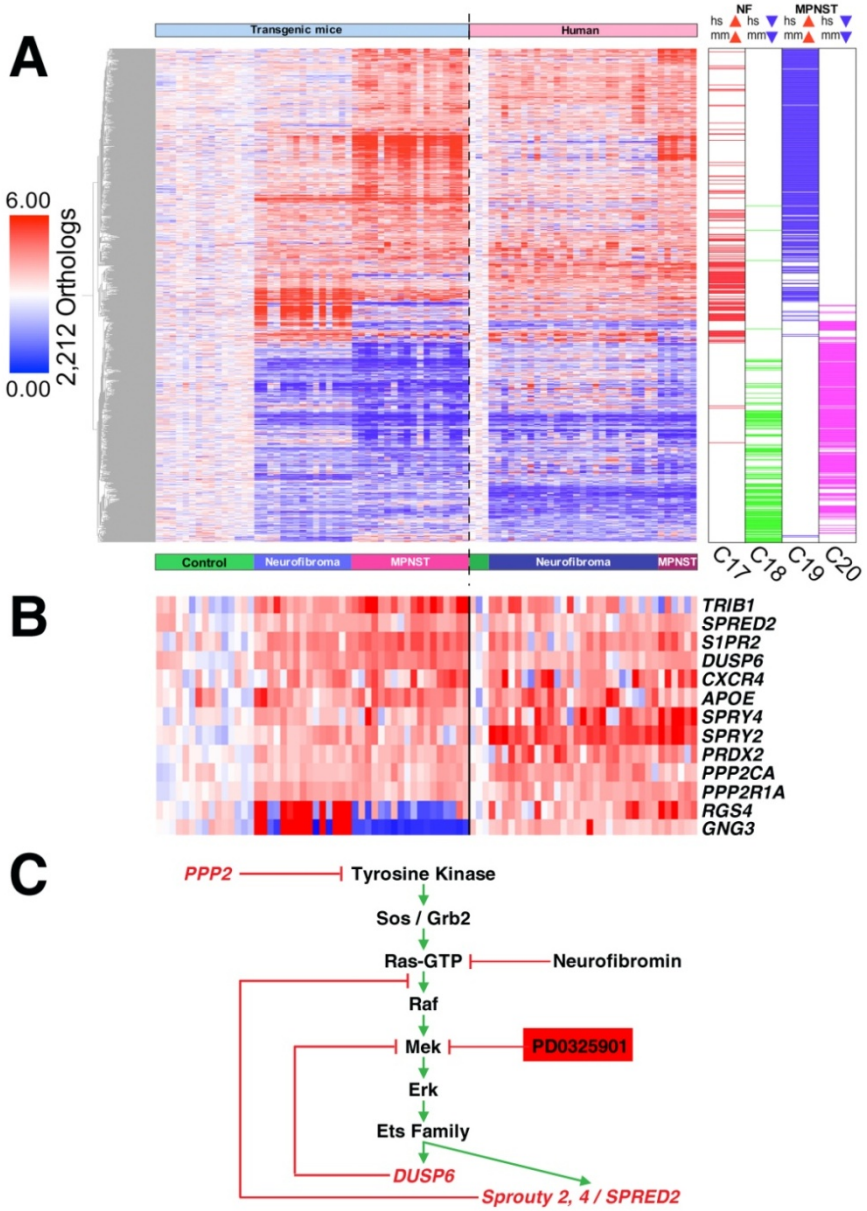

Supplemental Figure S1. ***Gene expression patterns in mouse and human NF1 tumors highlight altered transcriptional regulation of genes associated with Raf/MEK/ERK signal transduction.*** **(A)** Heat map of 2,212 gene orthologs with similar expression profiles in GEM model neurofibromas and human neurofibromas, or GEM model MPNSTs and human MPNSTs relative to normal human or control mouse peripheral nerve. Red = up-regulation; blue = down-regulation. Vertical bars to the right of the heat map show clusters (C17 – C20) of gene orthologs with similar expression patterns as indicated in each species (red arrow: over-expression; blue arrow: under-expression; hs = Homo sapiens; mm = Mus musculus). **(B)** Hierarchical clustering of genes associated with Raf/MEK/ERK (Also known as the MAPK) pathway signal transduction from (A) as identified by connectivity networking. **(C)** Ras/Raf/Mek/Erk signal transduction pathway including negative regulation of Ras-GTP by neurofibromin, MEK inhibition by the PD0325901 clinical compound, and known negative feedback by proteins with up-regulated gene expression from (B).

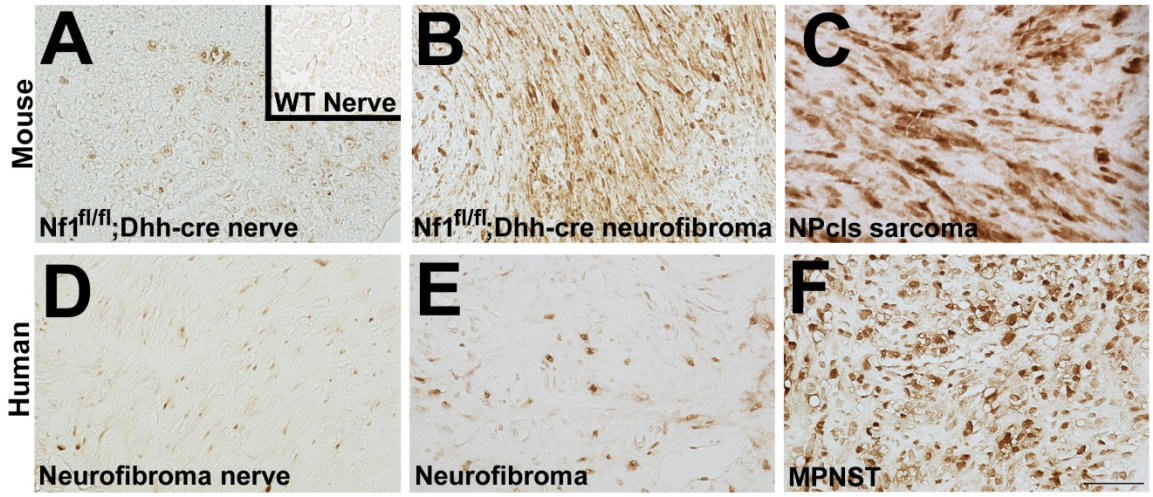

Supplemental Figure S2: ***ERK signaling is activated in neurofibromas and MPNSTs.***
(A - F) Brown staining indicates detection of phosphorylated (p)-ERK in paraffin tissue sections. Low levels of p-ERK are detected in **(A)** *Nf1$^{fl/fl}$;Dhh-cre* and wild type (inset) adult mouse nerve and **(D)** human neurofibroma-associated peripheral nerve; Intermediate levels of p-ERK are detected in **(B)** *Nf1$^{fl/fl}$;Dhh-cre* neurofibroma and **(E)** human neurofibroma; High levels of p-ERK are detected in **(C)** GEM model NPcis sarcoma similar to MPNST and **(F)** human MPNST. Human neurofibroma nerve **(D)** and neurofibroma **(E)** were taken from the same tissue section and are representative; the cellularity is greater in neurofibroma **(E)** than normal nerve **(D)** as is the intensity per cell. Scale bar = 50 μm; scale bar in **(F)** applies to **(A – F)**. Double-labeling with p-ERK and Schwann cell (CNPase) or endothelial cell (MECA) markers indicated both Schwann cells and endothelial cells had activated ERK signaling, in neurofibromas and MPNSTs (data not shown). In *Nf1$^{fl/fl}$;Dhh-cre* neurofibromas, 35% of the CNPase+ cells (Schwann cells) were p-ERK+. This is consistent with the population of Schwann cells that express an EGFP marker for *Nf1* loss (~45%) in *Nf1$^{fl/fl}$;Dhh-cre* mice (1). In MPNST xenografts, 31% of CNPase+ cells were p-ERK+. Approximately half of MECA1+ endothelial cells were p-ERK+ in neurofibromas (55%) and MPNSTs (58%), possibly contributing to documented effects in tumor vasculature.

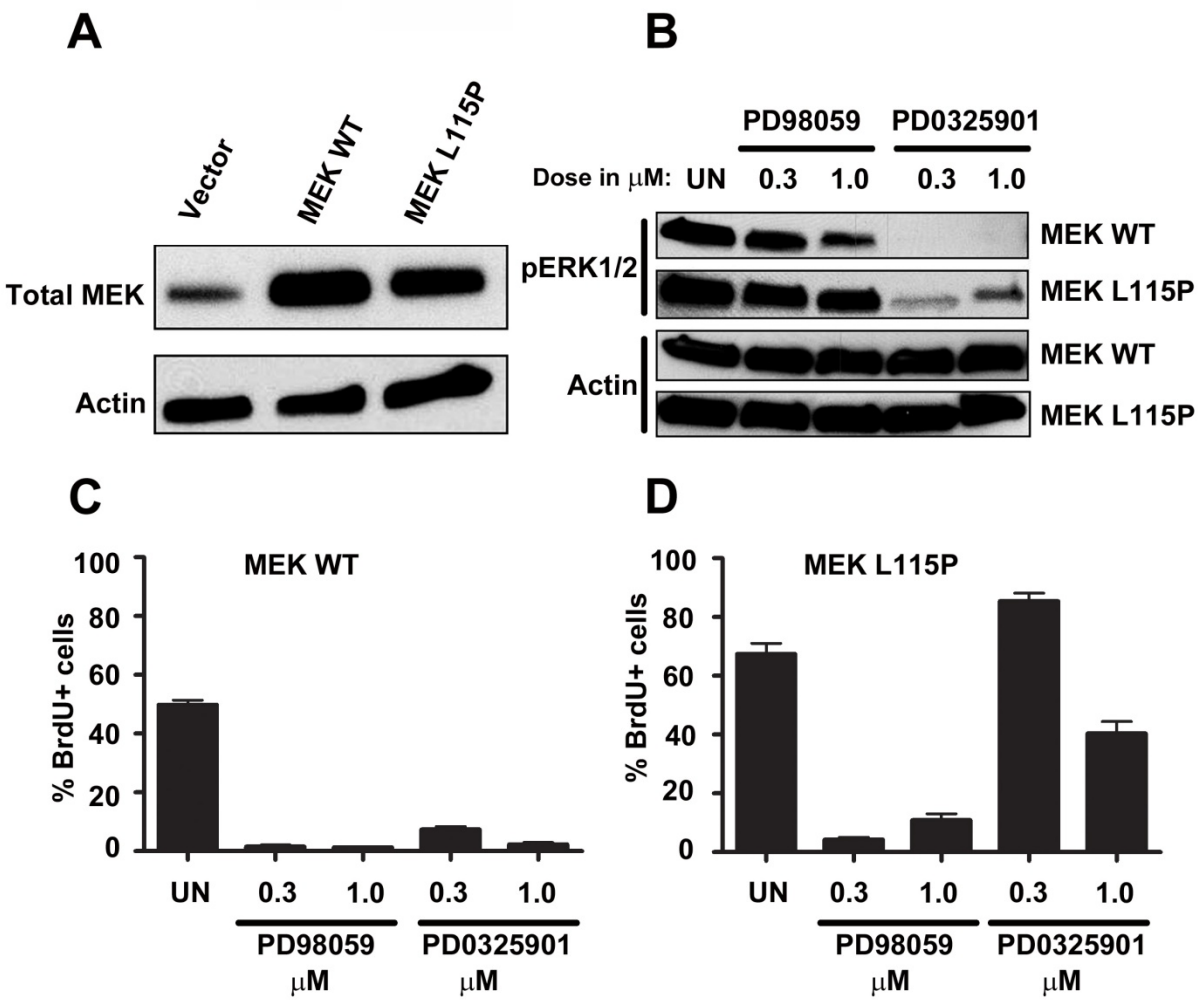

Supplemental Figure S3: MEK inhibition is the biological effect of PD0325901 in NF1 tumor cells. (A) Western blot analysis showing overexpression of wild type (MEK WT) or mutant (MEKL115P) MEK proteins. Anti-β-actin was used as a loading control. (B) Western blot analysis of levels of pERK1/2 in cells expressing MEK WT or MEK L115P following a 24 hour treatment with PD98059 or PD0325901 at two doses. Note that PD0325901 is more potent than PD98059. Cells expressing the mutant MEK maintain ERK phosphorylation in the presence of PD0325901 demonstrating the specificity of this inhibitor for the MEK allosteric site. Similar results were obtained following a 2h stimulation. (C) Quantitation of BrdU positive MPNST 8814 cells expressing MEK WT. A decrease in cell proliferation is present at two doses of each MEK inhibitor. (D) Quantification of BrdU positive MPNST 88-14 cells expressing MEK L115P. Cells expressing the mutant MEK are refractory to PD0325901. Error bars represent mean +/- standard error of the mean of four replicates.

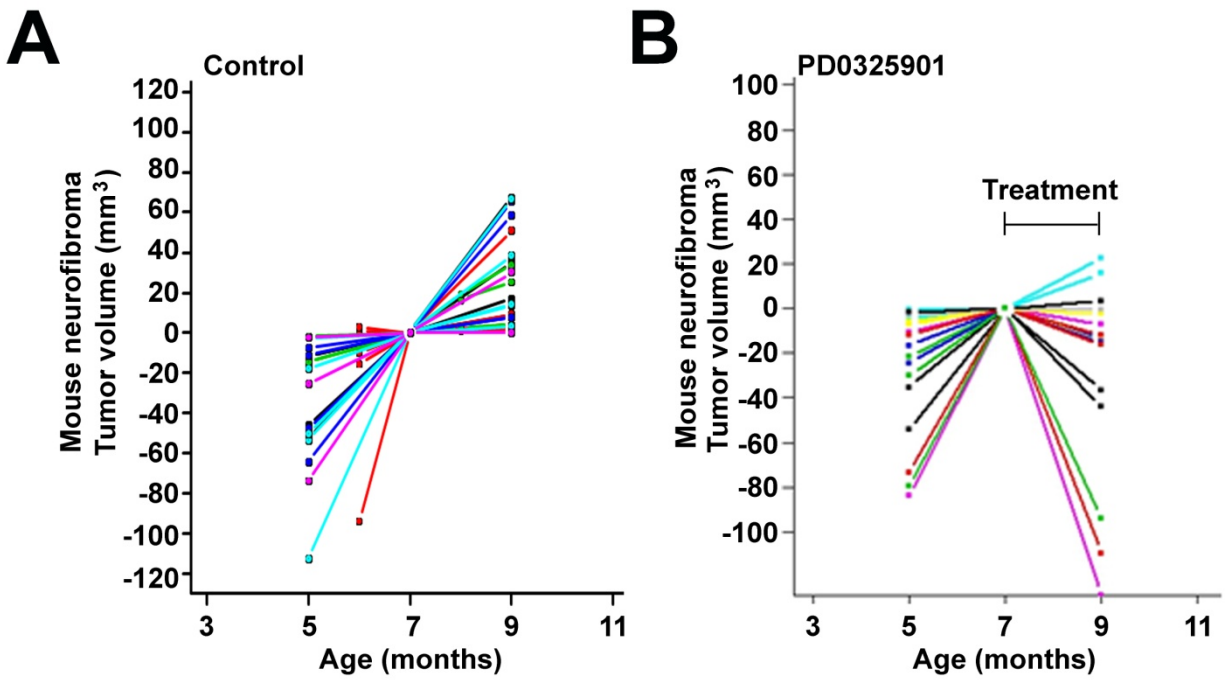

Supplemental Figure S4 (related to Figure 2). $Nf1^{flox/flox}$;DhhCre neurofibroma volume is reduced by PD0325901. Volumetric measurements of vehicle-treated **(G)** or PD032901-treated **(H)** *$Nf1^{flox/flox}$;DhhCre* mice indicate a median decrease in neurofibroma volume of 17% (range 0 – 59%); no control tumors regressed ($p<0.001$ calculated by Mixed Effects Model Analysis). The x-axis shows time in months and the y-axis plexiform neurofibroma tumor volume in mm^3 quantified by measurements of MRI scans.

Supplemental Methods

Microarray hybridization. The human NF1 tumor data set consisted of 3 normal nerves, 13 dermal neurofibromas, 13 plexiform neurofibromas and 6 MPNSTs; samples (except for normal nerves) were previously described (2). The GEM Nf1 model tumor data set consisted of 15 littermate control nerves encompassing 3 genotypes (5 P0CreB, 5 Nf1 flox/flox, 5 Nf2 flox/flox), 15 GEM model neurofibromas encompassing 3 genotypes (4 DhhCre; Nf1 flox/-, 7 DhhCre; Nf1 flox/flox, 4 P0CreB; Nf1 flox/flox) and 18 GEM model MPNSTs encompassing 5 genotypes (5 P0CreB; Nf1 flox/flox; Nf2 flox/+, 3 P0CreB; Nf2 flox/flox, 3 P0CreB; Nf1 flox/+; Nf2 flox/flox, 3 P0CreB; Nf2 flox/flox; p53+/-, 4 NPcis) (**Supplemental Table S1**). The entire microarray dataset will be available in the GEO database (http://www.ncbi.nlm.nih.gov/geo/).

Orthologous gene expression filtering. To identify similarly regulated transcripts, expression level filtering on log scale normalized intensities was used to identify and pool orthologous genes up-regulated > 1.2 or < 0.8 in 18 of 26 human neurofibroma samples or 4 of 6 MPNST samples, and > 1.2 or < 0.8 in 11 of 15 GEM model neurofibroma or 13 of 18 GEM model MPNST samples.

Cross-species data set integration. Statistical comparisons were made between mouse sample types (i.e. nerve vs. neurofibroma vs. MPNST), not GEM genotype, to identify genes conserved among GEM Nf1 models and align comparisons made between human NF1 tumors and normal peripheral nerve. We combined genes differently expressed in either species on an orthologous gene platform based on gene ortholog matching across species. Microarray probes from each array platform were mapped to common gene orthologs identified in the Mouse Genome Informatics (MGI) Database (Human and Mouse Orthology, Jul 16, 2009) (3, 4).

Functional annotation and gene-based associations. Statistically enriched Gene Ontologies, KEGG pathways and BioCarta pathways ($P \leq 0.05$) were identified using the Database for Annotation, Visualization and Integrated Discovery (DAVID) 2008 at the National Institute of Allergy and Infectious Diseases (NIAID), National Institutes of Health (NIH) (5).

Additional gene-based associations were identified using GATACA (http://gataca.cchmc.org/gataca/).

Gene association network. Co-functional enrichment analysis of gene ortholog clusters C17 – C33 was performed using ToppGene (6). Gene orthologs and associated ontologies, pathways, transcription factor binding sites (TFBS), cytobands, protein domains, drug-disease associations and gene set-disease associations were used to construct a gene association network. Cytoscape was used to visualize the gene association network, consisting of 2,653 nodes and 7,938 edges (7). We used the yFiles organic layout to arrange the network independent of biological attributes.

Gene expression microarray data generation and normalization. Total RNA was isolated from human nerves and tumors as described previously (2). Total RNA was isolated from mouse nerves and tumors using the Qiagen fibrous tissue protocol (Qiagen, Inc. Valencia, CA). Microrarray hybridizations of mouse samples were conducted in 10 independent batches as space allowed, each batch including at least one sample from each sample type. To control for batch variation, a common mouse embryo reference sample was included in each batch hybridization. For comparison with previously generated human tumor data using a universal human reference sample (2), microarray hybridization of human nerve samples was conducted in an independent batch including the universal human reference sample. Expression profiles were generated using Affymetrix HG-U133 plus 2 and MOE430 2.0 oligonucleotide microarrays. Affymetrix Microarray Suite 5.0 was used to generate 'CEL' files for each sample that were normalized using the Robust Multichip Analysis (RMA) algorithm as implemented in Bioconductor/R (8). Affymetrix probes were remapped to the latest annotated RefSeq genes (version 11.0.1) (9). CEL files were imported into GeneSpring GX v7.3.1; Agilent Technologies for data analysis. Prior to statistical comparisons between sample types, the normalized gene expression level value for each transcript in each sample was set to its ratio relative to the expression of that transcript's measurement in the appropriate reference sample, mouse or

human. The normalized gene expression level value for each transcript in each sample was then set to its ratio relative to the median expression of that transcript's measurements across control mouse or human nerve samples.

Statistical analyses of gene expression microarray data. All statistical comparisons and data visualization were performed using GeneSpring GX v7.3.1 (Agilent Technologies). For the GEM models, 14,480 transcripts were identified as differentially expressed using an ANOVA ($P \leq 0.05$) between control mice, neurofibroma models and MPNST models. For the human tumors, 7,174 transcripts were identified as differentially expressed using an ANOVA ($P \leq 0.05$) between normal nerves, neurofibromas and MPNSTs. All statistical tests were corrected for multiple testing effects by applying the Benjamini and Hochberg false discovery rate correction (10).

Ortholog gene mapping. Two data sources were used for orthogonal mapping between mouse and human genes Affymetrix probe sequence data (Human affx_probe.fasta downloaded on 2009-07-16 and Mouse affx_probe.fasta downloaded on 2009-07-16) and Refseq RNA sequence data (human.rna.gbff.gz downloaded on 2009-07-16 and mouse.rna.gbff.gz downloaded on 2009-07-16). These files were used to extract transcript sequences, probe sequences and probe sets. We validated probe sets by verifying that probes match the Refseq gene sequence, are unique across all genes and have a valid probe ratio ≥ 50%. Validated probe sets were then used to form the Orthogonal Mapping for the Human and Mouse species, utilizing The Jackson Laboratory's Human vs. Mouse Orthology (HMD_Human5.rpt generated 2009-07-16). Once the data was integrated, we focused on 8,974 gene orthologs statistically different in at least one of the two species *and* present in both mouse and human data sets.

To identify inversely expressed transcripts, expression level filtering on log scale normalized intensities was used to identify and pool orthologous genes up-regulated > 1.2 or down-regulated < 0.8 in 18 of 26 human neurofibroma samples but down-regulated < 0.8 or up-

regulated > 1.2 in 11 of 15 GEM model neurofibroma samples, and genes up-regulated > 1.2 or down-regulated < 0.8 in 4 of 6 human MPNST samples but down-regulated < 0.8 or up-regulated > 1.2 in 13 of 18 GEM model MPNST samples.

To identify uniquely regulated human transcripts, we isolated those gene orthologs statistically different from the human data set but not differentially expressed in the mouse data set or in the list of gene orthologs similarly or inversely expressed. For mouse, we isolated those gene orthologs statistically different from the mouse data set but not differentially expressed in the human data set or in the list of gene orthologs similarly or inversely expressed.

Cross-species data integration. A total of 7,174 transcripts were differentially expressed (ANOVA, FDR ≤ 0.05) in 26 neurofibromas and/or 6 MPNSTs relative to 3 normal human nerves. In our mouse model data set, a total of 14,480 transcripts were differentially expressed (ANOVA, FDR ≤ 0.05) in 15 mouse neurofibromas from 3 GEM Nf1 models and/or 18 mouse MPNSTs from 5 GEM Nf1 models relative to 15 control nerves from 3 GEM models. Following cross-species integration, 8,974 gene orthologs were significantly differentially expressed in either the mouse or human data set and present on the Affymetrix Human Genome U133 Plus 2.0 Array and Mouse Genome MOE430 2.0 cDNA arrays. For mouse, human and cross-species analysis, hierarchical tree clustering identified major patterns of gene expression; we assigned transcripts to each using k-means clustering. For the cross-species analysis, we used ToppGene and the Gene Set Enrichment Algorithm to identify enriched functional categories within each cluster (6). We queried transcripts from each cluster for relative enrichment of Gene Ontologies and signaling pathways using the Database for Annotation, Visualization and Integrated Discovery (DAVID) 2008(5). We also used GATACA (Gene Associations To Anatomy and Clinical Abnormalities), a web accessible database that can be used to identify literature-based gene associations, to prioritize relevant genes listed within each cluster based upon known association with neurofibromatosis, NF1, neurofibroma, MPNST, nerve or peripheral nervous system (http://gataca.cchmc.org/gataca/). Gene orthologs

uniquely expressed in either species and excluding those (i) statistically differentially expressed in the other species and (ii) similarly (Supplemental Figure S1) or inversely expressed between GEM Nf1 models and human NF1 tumors, 309 gene orthologs were uniquely expressed in human NF1 tumors and 4,377 gene orthologs were uniquely expressed in GEM Nf1 models. Some apparent differences between species may be exaggerated as we are limited by (i) the presence of genes on the Affymetrix platform that have an ortholog, (ii) the subset of gene orthologs that passed our validation steps for uniqueness and specificity and (iii) genes that are documented in the mouse genome database.

Immunohistochemistry. Paraffin sections were deparaffinized, hydrated and transferred to 0.1M citrate buffer (pH 6.0) for antigen retrieval. Slides were boiled for 10 minutes in citrate buffer, cooled at room temperature for 30 minutes, rinsed in water twice and in PBS 3 times. Sections were quenched with 3% hydrogen peroxide for 10 minutes, rinsed in PBS, and blocked in 10% normal goat serum with 0.3% Triton-X-100. Sections were incubated overnight in primary antibody diluted in block; rabbit pERK (Cell Signaling #4370; 1:200). Sections were then incubated in goat anti-rabbit biotinylated secondary antibodies.

Transient transfection of MPNST cells. *NF1* mutant human MPNST ST8814 cells were transiently transfected with plasmids expressing either wild type (WT) MEK or mutant MEK L115P (a gift from Dr. Kevin Shannon, UCSF, San Francisco, CA) by electroporation using an Lonza Nucleofector (package V02.15). We transfected 1ug plasmid DNA per 10^6 cells in 100ul of buffer SG (Lonza Amaxa SG Cell Line Buffer) using the Lonza Nucleofector program EN150. Cells were plated in DMEM with 10% FBS, allowed to recover for 24 hours recovery, serum starved overnight in DMEM with 0.1% FBS, and then stimulated with 10% FBS and the MEK inhibitors overnight. For detection of proliferating cultured cells, anti-BrdU (Abcam) staining was performed on MPNST cells (n=4 per condition) fixed on Lab-Tek chamber slides. The numbers of BrdU+ and DAPI+ cells were counted in sixteen 10x fields from 4 replicate wells. Primary antibodies (Cell Signaling, Danvers, MA) for Westerns from RIPA lysates from cultured cells

were used at the following dilutions: MEK #9122 (1:1000), pERK 1/2 #4370 (1:2000), Actin #5125 (1:5000).

Supplemental References

1. Wu, J., Williams, J.P., Rizvi, T.A., Kordich, J.J., Witte, D., Meijer, D., Stemmer-Rachamimov, A.O., Cancelas, J.A., and Ratner, N. 2008. Plexiform and dermal neurofibromas and pigmentation are caused by Nf1 loss in desert hedgehog-expressing cells. *Cancer Cell* 13:105-116.
2. Miller, S.J., Jessen, W.J., Mehta, T., Hardiman, A., Sites, E., Kaiser, S., Jegga, A.G., Li, H., Upadhyaya, M., Giovannini, M., et al. 2009. Integrative genomic analyses of neurofibromatosis tumours identify SOX9 as a biomarker and survival gene. *EMBO Mol Med* 1:236-248.
3. Eppig, J.T., Bult, C.J., Kadin, J.A., Richardson, J.E., Blake, J.A., Anagnostopoulos, A., Baldarelli, R.M., Baya, M., Beal, J.S., Bello, S.M., et al. 2005. The Mouse Genome Database (MGD): from genes to mice--a community resource for mouse biology. *Nucleic Acids Res* 33:D471-475.
4. Kaiser, S., Park, Y.K., Franklin, J.L., Halberg, R.B., Yu, M., Jessen, W.J., Freudenberg, J., Chen, X., Haigis, K., Jegga, A.G., et al. 2007. Transcriptional recapitulation and subversion of embryonic colon development by mouse colon tumor models and human colon cancer. *Genome Biol* 8:R131.
5. Huang da, W., Sherman, B.T., and Lempicki, R.A. 2009. Systematic and integrative analysis of large gene lists using DAVID bioinformatics resources. *Nat Protoc* 4:44-57.
6. Chen, J., Xu, H., Aronow, B.J., and Jegga, A.G. 2007. Improved human disease candidate gene prioritization using mouse phenotype. *BMC Bioinformatics* 8:392.

7. Cline, M.S., Smoot, M., Cerami, E., Kuchinsky, A., Landys, N., Workman, C., Christmas, R., Avila-Campilo, I., Creech, M., Gross, B., et al. 2007. Integration of biological networks and gene expression data using Cytoscape. *Nat Protoc* 2:2366-2382.

8. Irizarry, R.A., Hobbs, B., Collin, F., Beazer-Barclay, Y.D., Antonellis, K.J., Scherf, U., and Speed, T.P. 2003. Exploration, normalization, and summaries of high density oligonucleotide array probe level data. *Biostatistics* 4:249-264.

9. Dai, M., Wang, P., Boyd, A.D., Kostov, G., Athey, B., Jones, E.G., Bunney, W.E., Myers, R.M., Speed, T.P., Akil, H., et al. 2005. Evolving gene/transcript definitions significantly alter the interpretation of GeneChip data. *Nucleic Acids Res* 33:e175.

10. Benjamini, Y., Drai, D., Elmer, G., Kafkafi, N., and Golani, I. 2001. Controlling the false discovery rate in behavior genetics research. *Behav Brain Res* 125:279-284.